Spectroscopy and Electrochemistry of Cytochrome P450 BM3-Surfactant Film Assemblies

Andrew K. Udit,*,[†] Katharine D. Hagen,[†] Peter J. Goldman,[†] Andrew Star,[†] James M. Gillan,[†] Harry B. Gray,[‡] and Michael G. Hill*,[†]

Contribution from the Department of Chemistry, Occidental College, Los Angeles, California 90041, and Division of Chemistry and Chemical Engineering, California Institute of Technology, Pasadena, California 91125

Received March 20, 2006; E-mail: udit@oxy.edu; mgh@oxy.edu

Abstract: We report analyses of electrochemical and spectroscopic measurements on cytochrome P450 BM3 (BM3) in didodecyldimethylammonium bromide (DDAB) surfactant films. Electronic absorption spectra of BM3−DDAB films on silica slides reveal the characteristic low-spin Fe^{III} heme absorption maximum at 418 nm. A prominent peak in the absorption spectrum of BM3 Fe^{II}−CO in a DDAB dispersion is at 448 nm; in spectra of aged samples, a shoulder at ~420 nm is present. Infrared absorption spectra of the BM3 Fe^{II}−CO complex in DDAB dispersions feature a time-dependent shift of the carbonyl stretching frequency from 1950 to 2080 cm^{-1}. Voltammetry of BM3-DDAB films on graphite electrodes gave the following results: $Fe^{III/II}$ $E_{1/2}$ at −260 mV (vs SCE), ~300 mV positive of the value measured in solution; ΔS°_{rc}, ΔS°, and ΔH° values for water-ligated BM3 in DDAB are −98 $J mol^{-1} K^{-1}$, −163 $J mol^{-1} K^{-1}$, and −47 $kJ mol^{-1}$, respectively; values for the imidazole-ligated enzyme are −8 $J mol^{-1} K^{-1}$, −73 $J mol^{-1} K^{-1}$, and −21 $kJ mol^{-1}$. Taken together, the data suggest that BM3 adopts a compact conformation within DDAB that in turn strengthens hydrogen bonding interactions with the heme axial cysteine, producing a P420-like species with decreased electron density around the metal center.

Introduction

The cytochromes P450 (P450s) are heme-thiolate monooxygenases that perform critical functions in living systems.[1] Owing to their importance in medicine and pharmacology,[2] as well as their potential to catalyze challenging oxidations for commercial chemical synthesis,[3] there is great interest in capturing P450 activity in vitro. However, the many attempts to replicate this system in vitro have been only marginally successful, owing to the intricate electron transfer (ET) machinery required for P450 catalysis.[4−9]

Electrochemical methods are perhaps the simplest way of providing P450s with reducing equivalents for catalysis.[10] In particular, following Rusling's pioneering work,[11] surfactant films on carbon surfaces have been employed by many investigators to achieve electronic coupling between heme proteins and electrodes.[12−23] The surfactant is deposited onto the electrode, resulting in the formation of bilayers, vesicles, and micelles (depending on the surfactant, the surface, and ionic strength);[24−27] protein molecules incorporated into the film are embedded within hydrophobic regions.[28] This methodology has proven particularly effective for P450s, which possess deeply

† Occidental College.

‡ California Institute of Technology.

(1) Ortiz de Montellano, P. R. *Cytochrome P450: Structure, Mechanism, and Biochemistry*, 2nd ed.; Plenum Press: New York, 1995.

(2) Guengerich, F. P. *Molecular Interventions* **2003**, *3*, 194−204.

(3) Peters, M. W.; Meinhold, P.; Glieder, A.; Arnold, F. H. *J. Am. Chem. Soc.* **2003**, *125*, 13442−13450.

(4) Estabrook, R.; Faulkner, K.; Shet, M.; Fisher, C. *Methods Enzymol.* **1996**, *272*, 44−51.

(5) Reipa, V.; Mayhew, M. P.; Vilker, V. L. *Proc. Natl. Acad. Sci. U.S.A.* **1997**, *94*, 13554−13558.

(6) Udit, A. K.; Hill, M. G.; Bittner, V. G.; Arnold, F. H.; Gray, H. B. *J. Am. Chem. Soc.* **2004**, *126*, 10218−10219.

(7) Shumyantseva, V.; Bulko, T.; Bachmann, T.; Bilitewski, U.; Schmid, R.; Archakov, A. *Arch. Biochem. Biophys.* **2000**, *377* (1), 43−48.

(8) Fantuzzi, A.; Fairhead, M.; Gilardi, G. *J. Am. Chem. Soc.* **2004**, *126*, 5040−5041.

(9) Munge, B.; Estavillo, C.; Schenkman, J. B.; Rusling, J. F. *ChemBioChem* **2003**, *4*, 82−89.

(10) Udit, A. K.; Gray, H. B. *Biochem. Biophys. Res. Commun.* **2005**, *338*, 470−476.

(11) Rusling, J. F. *Acc. Chem. Res.* **1998**, *31*, 363−369.

(12) Zhang, Z.; Nassar, A.-E.; Lu, Z.; Schenkman, J. B.; Rusling, J. F. *J. Chem. Soc., Faraday Trans.* **1997**, *93* (9), 1769−1774.

(13) Rusling, J. F.; Nassar, A.-E. F. *J. Am. Chem. Soc.* **1993**, *115*, 11891−11897.

(14) Zu, X.; Lu, Z.; Zhang, Z.; Schenkman, J. B.; Rusling, J. F. *Langmuir* **1999**, *15*, 7372−7377.

(15) Fleming, B. D.; Tian, Y.; Bell, S. G.; Wong, L.; Urlacher, V.; Hill, H. A. O. *Eur. J. Biochem.* **2003**, *270*, 4082−4088.

(16) Aguey-Zinsou, K.; Bernhardt, P. V.; Voss, J. J. D.; Slessor, K. E. *Chem. Commun.* **2003**, 418−419.

(17) Bayachou, M.; Boutros, J. A. *J. Am. Chem. Soc.* **2004**, *126*, 12722−12723.

(18) Udit, A. K.; Belliston-Bittner, W.; Glazer, E. C.; Nguyen, Y. H. L.; Gillan, J. M.; Hill, M. G.; Marletta, M. A.; Goodin, D. B.; Gray, H. B. *J. Am. Chem. Soc.* **2005**, *127*, 11212−11213.

(19) Blair, E.; Greaves, J.; Farmer, P. J. *J. Am. Chem. Soc.* **2004**, *126*, 8632−8633.

(20) Farmer, P.; Lin, R.; Bayachou, M. *Comments Inorg. Chem.* **1998**, *20*, 101−120.

(21) Liu, H.; Wang, L.; Hu, N. *Electrochim. Acta* **2002**, *47*, 2515−2523.

(22) Ma, H.; Hu, N. *Anal. Lett.* **2001**, *34* (3), 339−361.

(23) Shukla, A.; Gillam, E. M.; Mitchell, D. J.; Bernhardt, P. V. *Electrochem. Commun.* **2005**, *7*, 437−442.

(24) Lange, K. R. *Surfactants: A Practical Handbook*; Hanser Gardner Publications: Cincinnati, OH, 1999.

(25) Jaramillo, A.; Marino, A.; Brajter-Toth, A. *Anal. Chem.* **1993**, *65*, 3441−3446.

(26) Manne, S.; Cleveland, J. P.; Gaub, H. E.; Stucky, G. D.; Hansma, P. K. *Langmuir* **1994**, *10*, 4409−4413.

(27) Wanless, E. J.; Ducker, W. A. *J. Phys. Chem.* **1996**, *100*, 3207−3214.

buried hemes. Notably, some aspects of the P450-surfactant system remain puzzling. Most prominent is the large heme potential shift that accompanies immobilization of the protein within the film on the electrode surface. Additional points of interest are the greatly enhanced ET rates within the film and the relatively small (cf. solution) potential shift of the heme $Fe^{III/II}$ redox couple in the presence of carbon monoxide.[29,30] Further underscoring these points is the poor ability of P450 (cf. native activity) to support substrate oxidation, despite enhanced ET. Taken together, these observations could indicate that the proteins are structurally perturbed within the film.[31–34] However, we emphasize that two key spectroscopic results, namely, the peak positions in the spectra of P450-surfactant assemblies on transparent substrates,[35] as well as the observed 450 nm signature of the Fe^{II}–CO enzyme redispersed into solution from electrode surfaces,[12] support a native-like P450 conformation in the film.

We are investigating the spectroscopic and redox properties of cytochrome P450 from *Bacillus megaterium* (BM3) within didodecyldimethylammonium bromide (DDAB) films.[15,36] Here we report results from electronic and infrared (IR) absorption spectroscopic measurements as well as electrochemical data that support a model that features collapse of the protein structure around the heme triggered by (1) heme dehydration and (2) tightening of the hydrogen bonding (H-bonding) network within the polypeptide.

Results

Electronic Absorption Spectroscopy. To investigate protein integrity within surface-confined films, we prepared BM3−DDAB films on fused silica slides and recorded the electronic absorption spectrum. The slides were cleaned with "piranha" solution and then coated with (3-mercapto)trimethoxysilane to enhance film adhesion.[37] A BM3−DDAB mixture was then applied to the surface and allowed to dry slowly under water-saturated air overnight. The resulting films were sufficiently transparent and stable to allow characterization by UV−visible spectroscopy. Reproducible spectra were obtained on these slides: in a typical spectrum, a distinct peak (λ_{max}) is observed at 418 nm, similar to the position of the Soret band in the spectrum of water-ligated low-spin Fe^{III} BM3 in solution (Figure 1). This result is consistent with prior work in which the solution-like heme Soret bands of myoglobin[20] and P450[35] were observed using similar transparent substrates.

Perturbations to the electronic structure of the BM3 heme within DDAB dispersions were probed using the BM3
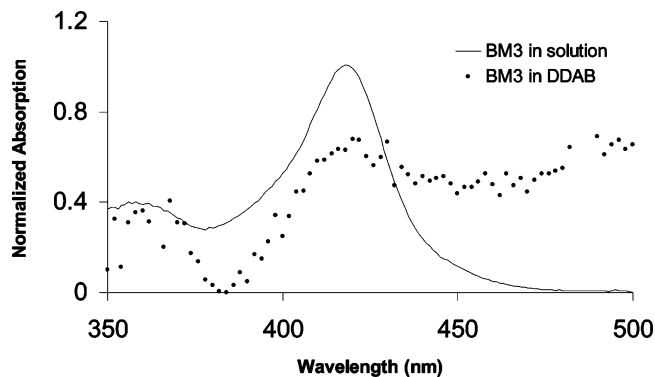

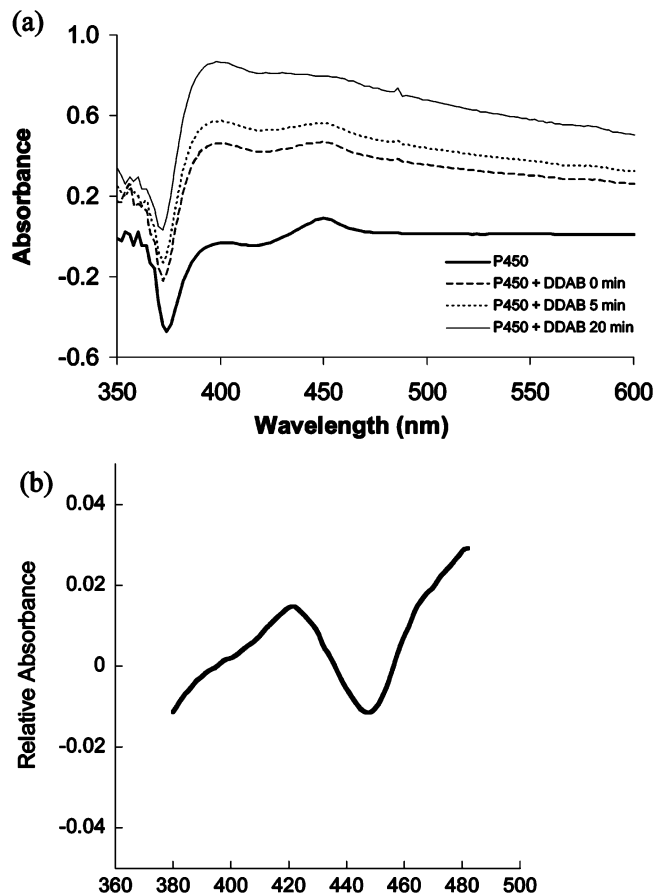**Figure 1.** Absorption spectra of BM3 in solution and BM3 in DDAB on silica. Both spectra display λ_{max} at 418 nm.

Figure 2. (a) Absorption spectra of the BM3 Fe^{II}−CO complex (2 μM) in a DDAB dispersion (40 μM) at ambient temperature are shown. (b) Difference spectrum of Fe^{II}−CO BM3 (1.3 μM) in a DDAB dispersion (40 μM) at ambient temperature 2 min after mixing the solution. The buffer was 50 mM KP_i/50 mM KCl/pH 7.

Fe^{II}−CO complex (λ_{max} = 448 nm). Figure 2a shows a series of spectra taken from a dispersion of 40 μM DDAB and 2 μM BM3 Fe^{II}−CO in buffer.[38] From these spectra, it can be seen that at short time intervals there is no significant change in the absorption spectrum, while longer times (>∼20 min) reveal a shoulder at ∼420 nm. A difference spectrum (Figure 2b) recorded after 2 min of incubating 1.3 μM BM3 Fe^{II}−CO and 40 μM DDAB clearly demonstrates the shift in absorption maximum from 448 to 422 nm. Notably, absorption of the P450

(28) Protein can be incorporated in several ways, including co-deposition with the surfactant and soaking the surfactant-coated electrode in a protein solution.

(29) For comparison, the $Fe^{III/II}$ redox potential of rabbit liver P450 is shifted +180 mV in the presence of CO. See ref 30.

(30) Guengerich, F. P.; Ballou, D. P.; Coon, M. J. *J. Biol. Chem.* **1975**, *250*, 7405−7411.

(31) Some investigations with myoglobin have suggested that the protein may denature within surfactant film assemblies under certain conditions (refs 32 and 33), while other studies strongly indicate that the native structure is intact (summarized in ref 34).

(32) Tofani, L.; Feis, A.; Snoke, R. E.; Berti, D.; Baglioni, P.; Smulevich, G. *Biophys. J.* **2004**, *87*, 1186−1195.

(33) de Groot, M. T.; Merkx, M.; Koper, M. T. M. *J. Am. Chem. Soc.* **2005**, *127*, 16224−16232.

(34) Guto, P. M.; Rusling, J. F. *Electrochem. Commun.* **2006**, *8*, 455−459.

(35) Immoos, C. E.; Chou, J.; Bayachou, M.; Blair, E.; Greaves, J.; Farmer, P. J. *J. Am. Chem. Soc.* **2004**, *126*, 4934−4942.

(36) Udit, A. K.; Hindoyan, N.; Hill, M. G.; Arnold, F. H.; Gray, H. B. *Inorg. Chem.* **2005**, *44*, 4109−4111.

(37) Goss, C. A.; Charych, D. H.; Majda, M. *Anal. Chem.* **1991**, *63*, 85−88.

(38) The solution became increasingly turbid with time, making it difficult to record consecutive spectra with a consistent baseline.
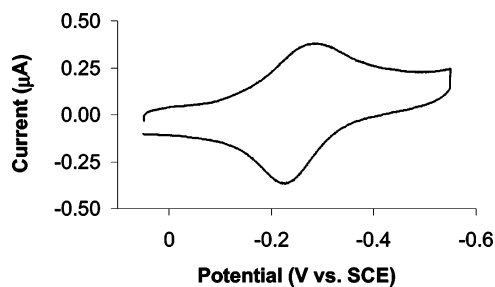
Figure 3. Cyclic voltammogram of BM3 in DDAB on basal plane graphite at 25 mV/s and 21.6 °C in 50 mM KP$_i$/50 mM KCl/pH 7 buffer.

ferrous-carbonyl complex at 420 nm has been ascribed to a biologically inactive form of the enzyme,[39] possibly deriving from enhanced hydrogen bonding to (or protonation of) the heme proximal thiolate ligand.[40,41]

Absorption spectra of free heme (5 μM) in buffer were also recorded in the presence and absence of DDAB (40 μM) (Figure S1). In the presence of DDAB, the heme λ_{max} shifts to 398 nm with no apparent change with time.

Cyclic Voltammetry. A typical cyclic voltammogram of BM3 in DDAB on basal plane graphite (hydrophobic) electrodes recorded at 21.6 °C, 25 mV/s in buffer is shown in Figure 3. At slow scan rates, a well-defined, chemically reversible redox couple centered at −260 mV (vs SCE) is observed.[18,42] We have assigned this redox couple to the heme Fe$^{III/II}$ process. Consistent with other studies of heme-thiolate proteins in surfactant films,[15,17,35] the BM3 Fe$^{III/II}$ redox potential in DDAB is shifted to positive values relative to that determined in solution ($\Delta E°$ ≈ +300 mV).

Additional information concerning the nature of the BM3−DDAB−graphite system was obtained by evaluating the entropy change that accompanies ET at the heme reaction center ($\Delta S°_{rc}$). This parameter is accessible from the temperature dependence of the redox potential, which is conveniently measured using a nonisothermal electrochemical cell configuration:[43,44]

$$\Delta S°_{rc} = S°_{Fe(II)} - S°_{Fe(III)} = F(dE°/dT)$$

Voltammograms were recorded at 25 mV/s between 18.5 and 40 °C. As DDAB gel to liquid-crystal film transitions occur between 9 and 17 °C,[13] we performed our experiments above this range in order to eliminate phase-transition effects. The BM3 data reported below represent the results of at least four independent experiments for each set of conditions.

A plot of $E_{1/2}$ vs temperature reveals that the BM3 Fe$^{III/II}$ redox potential shifts approximately −1.02 mV/°C (Figure 4). The reaction entropy is equal to the slope of this line multiplied by the Faraday constant, which yields $\Delta S°_{rc} = -98$ J mol^{-1}

(39) Yu, C.-A.; Gunsalus, I. *J. Biol. Chem.* **1974**, *249*(1), 106−106.
(40) Martinis, S. A.; Blanke, S. R.; Hager, L. P.; Sligar, S. G.; Hoa, G. H. B.; Rux, J. J.; Dawson, J. H. *Biochemistry* **1996**, *35*, 14530−14536.
(41) Perera, R.; Sono, M.; Sigman, J. A.; Pfister, T. D.; Lu, Y.; Dawson, J. H. *Proc. Natl. Acad. Sci. U.S.A.* **2003**, *100* (7), 3641−3646.
(42) At faster scan rates a complex voltammogram with two cathodic peaks is observed. This behavior is analogous to that found for nitric oxide synthase in DDAB, indicative of water-free and water-bound hemes. See ref 18.
(43) DDAB is a permselective membrane, owing to its immobilized ammonium groups. Therefore, d$E°$/dT is additionally influenced by the entropy of ion transfer across the film/solution interface. Given the relatively low loading of R$_4$N$^+$ within the film, however, we estimate this contribution to be no more than several J mol^{-1} K^{-1}. We therefore present uncorrected values of $\Delta S°_{rc}$.
(44) Yee, E. L.; Cave, R. J.; Guyer, K. L.; Tyma, P. D.; Weaver, M. J. *J. Am. Chem. Soc.* **1979**, *101*, 1131−1137.
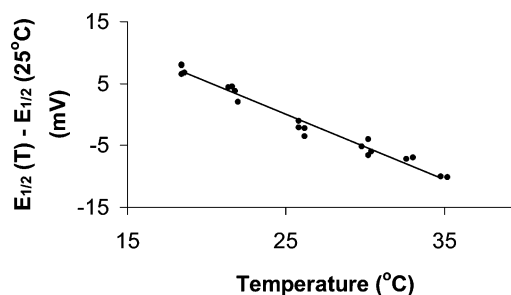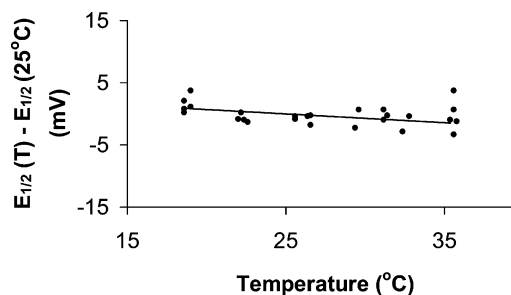
Figure 4. Temperature dependence of the BM3 water-ligated heme Fe$^{III/II}$ redox potential ($E_{1/2}$). Voltammograms were recorded at 25 mV/s in 50 mM KP$_i$/50 mM KCl/pH 7 buffer.

Table 1. Thermodynamic Parameters for Reduction of Heme Proteins

	$\Delta S°$ (J mol^{-1} K^{-1})	$\Delta H°$ (kJ mol^{-1})
BM3^a	−163	−47
BM3 + imidazole^a	−73	−21
myoglobin^{b,c}	−148	−38
horse heart cytochrome $c^{b,d}$	−127	−64

^{a} In DDAB film on graphite electrodes. ^{b} In solution. ^{c} See ref 51. ^{d} See ref 45.

Figure 5. Temperature dependence of the BM3 imidazole-ligated heme Fe$^{III/II}$ redox potential ($E_{1/2}$). Voltammograms were recorded at 25 mV/s in 50 mM KP$_i$/50 mM KCl/500 mM imidazole/pH 7 buffer.

K^{-1}.[45] Taking $S°$(H$_2$) = 130.4 J mol^{-1} K^{-1} and assigning $S°$(H$^+$) = 0,[45] we calculate an overall $\Delta S°$ for the complete cell reaction (adjusted to the NHE scale) of −163 J mol^{-1} K^{-1}. This value enables us to calculate $\Delta H°$ from the measured $E_{1/2}$ at 25 °C, which is −47 kJ mol^{-1}. Table 1 lists the calculated thermodynamic parameters for BM3 and values determined for other heme proteins.

We conducted analogous electrochemical experiments with BM3−DDAB films in the presence of 500 mM imidazole (Table 1). Imidazole replaces water as the heme axial ligand and, unlike water, remains bound to the heme in both Fe^{III} and Fe^{II} oxidation states.[46] Under these conditions, the Fe$^{III/II}$ $E_{1/2}$ (−247 mV vs SCE) is virtually temperature independent (−0.08 mV/°C, Figure 5). Calculated values for $\Delta S°_{rc}$, $\Delta S°$, and $\Delta H°$ are −8 J mol^{-1} K^{-1}, −73 J mol^{-1} K^{-1}, and −21 kJ mol^{-1}, respectively.

For comparison, we performed similar voltammetry experiments with free heme in DDAB on graphite. The complex voltammogram observed (Figure S2) made it difficult to appropriately assign $E_{1/2}$. Thus, we used the variation of the anodic peak potential ($E_{p,a}$) as a measure of the relative change in $E_{1/2}$ with temperature to estimate the thermal dependence of the heme Fe$^{III/II}$ process. The resulting data (Figure S3) were

(45) Taniguchi, V. T.; Sailasuta-Scott, N.; Anson, F. C.; Gray, H. B. *Pure Appl. Chem.* **1980**, 52, 2275−2281.
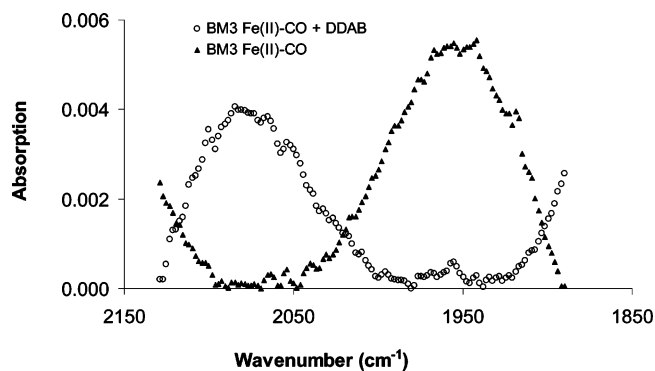(46) Dawson, J. H.; Andersson, L. A.; Sono, M. *J. Biol. Chem.* **1983**, *258*, 13637−13645.

Figure 6. Infrared absorption spectra of the BM3 $Fe^{II}-CO$ complex (∼60 uM) in the absence and presence of DDAB (2.5 mM) in 50 mM KP_i pH 7.

recorded from two independent experiments. $E_{p,a}$ varied with temperature according to 0.3 mV/°C, resulting in ΔS°_{rc} equal to 29 J mol^{-1} K^{-1}.

Infrared Absorption Spectroscopy. Absorption of IR radiation by the carbonyl ligand of the BM3 $Fe^{II}-CO$ adduct was used as a reporter for perturbations to the heme electronic structure within DDAB. Samples containing the BM3 $Fe^{II}-CO$ complex (∼60 μM) in the absence and presence of DDAB (2.5 mM) were prepared in 50 mM KP_i pH 7 buffer. The resulting spectra (Figure 6) yield λ_{max} at 1950 and 2080 cm^{-1} for BM3 $Fe^{II}-CO$ in the absence and presence of DDAB, respectively. We also recorded IR difference spectra that show the time-dependent shift of the BM3 $Fe^{II}-CO$ λ_{max} to higher frequency in the presence of DDAB, yielding a clear isosbestic point at 2020 cm^{-1}. Notably, the lower frequency absorption is consistent with other observations of the carbonyl stretching frequency of P450 $Fe^{II}-CO$ in solution.[47] In the case where DDAB is present, there appears to be a shift in the CO stretching frequency to a higher value.

Discussion

Electronic absorption spectroscopy provides a simple and informative tool for probing the P450 heme environment. Careful preparation of silica substrates allowed us to record the absorption spectrum of BM3 in DDAB on the transparent surface, which is virtually identical with the spectrum in solution and is characteristic of the six-coordinate water-ligated low-spin Fe^{III} heme. Absorption spectra recorded of the BM3 $Fe^{II}-CO$ complex in DDAB dispersions showed that the single λ_{max} of 448 nm evolved to a combination of 448 and 422 nm after a few minutes. Thus, it would appear that prolonged exposure of BM3 to DDAB in solution perturbs the structure of the protein-bound heme. Notably, absorption at 420 nm is indicative of P420, the little-understood biologically inactive form of P450 that may result from partial neutralization of the heme axial thiolate (possibly through protonation).[41] While neither of these experiments, BM3–DDAB films on silica or BM3 in DDAB dispersions, is fully representative of the P450–DDAB–graphite film system under investigation, where surface effects may play an undetermined role, it is clear that DDAB has the capacity to induce a P420-like state.

Additional information on the nature of immobilized BM3 was obtained from evaluating the change in entropy (ΔS°_{rc}) that accompanies ET at the reaction center. Since ΔS°_{rc} depends only on the variation of the measured potential with temperature, it represents the absolute entropy difference between the redox

states and can be used as an appropriate parameter to compare ET reactions between different complexes in different systems.[44] For water-ligated BM3, ΔS°_{rc} was estimated to be −98 J mol^{-1} K^{-1} and represents a significant decrease in entropy upon heme reduction. For protein structures, negative entropy changes are a result of the polypeptide adopting a more rigid conformation.[45,48] Specifically for the BM3−DDAB system, there are likely two factors contributing to this phenomenon. First, reduction of six-coordinate water-ligated Fe^{III} to Fe^{II} results in conversion to a five-coordinate heme due to the lability of the $Fe^{II}-OH_2$ bond.[49] An increase in hydrophobicity of the active site follows expulsion of the heme axial water ligand, likely leading to collapse of the protein around the heme.[48,50,51] Indeed, this "hydrophobic collapse" would lead to a compressed protein structure and subsequent loss in entropy. Examination of crystal structures provides some insight into the extent of dehydration that may occur; for example, P450 from *Pseudomonas putida* (CAM) has six water molecules within the active site and substrate access channel.[52] Since the extent of hydration is known to affect heme potentials,[53] it is likely that expulsion of water molecules from the active site of P450 would result in large positive heme potential shifts.

Second, the additional negative charge in the polypeptide matrix following heme reduction likely produces an overall tightening of the H-bonding network, thereby facilitating collapse of the protein and increasing the rigidity of the polypeptide.[45] Indeed, the change in enthalpy ($\Delta H^\circ = -47$ kJ mol^{-1}) indicates that the protein is stabilized in the reduced form, which is not surprising given the likely steric constraints of the surfactant environment.

We performed similar electrochemical experiments with BM3−DDAB films in the presence of 500 mM imidazole (Table 1), which replaces water as the heme axial ligand and remains heme-bound in both Fe^{III} and Fe^{II} oxidation states.[46] Under these conditions, ΔS°_{rc} is only −8 J mol^{-1} K^{-1}. Apparently, there is no significant change in entropy upon heme reduction with imidazole bound to the iron, in contrast to our findings for the water-ligated species. This difference is consistent with the likely structural rearrangements that accompany the redox reactions for the two different heme species: whereas reduction of a six-coordinate axially aquated heme triggers water dissociation and hydrophobic collapse, ET to an imidazole-bound heme produces no change in coordination, so there is minimal nuclear reorganization. The smaller loss in enthalpy (cf. water-ligated P450) with reference to our proposed model is consistent with protein stabilization owing to increased H-bonding, without the added benefit of polypeptide collapse around the active site due to the imidazole ligand remaining bound to the heme.

We suggest that enhanced H-bonding in the ferrous enzyme within DDAB will affect the heme axial thiolate, since this ligand is influenced by H-bonding interactions with the protein

(47) O'Keefe, D. H.; Ebel, R. E.; Peterson, J. A.; Maxwell, J. C.; Caughey, W. S. *Biochemistry* **1978**, *17* (26), 5845−5852.
(48) Grealis, C.; Magner, E. *Langmuir* **2003**, *19*, 1282−1286.
(49) Wilker, J. J.; Dmochowski, I. J.; Dawson, J. H.; Winkler, J. R.; Gray, H. B. *Angew. Chem., Int. Ed.* **1999**, *38*, 90−92.
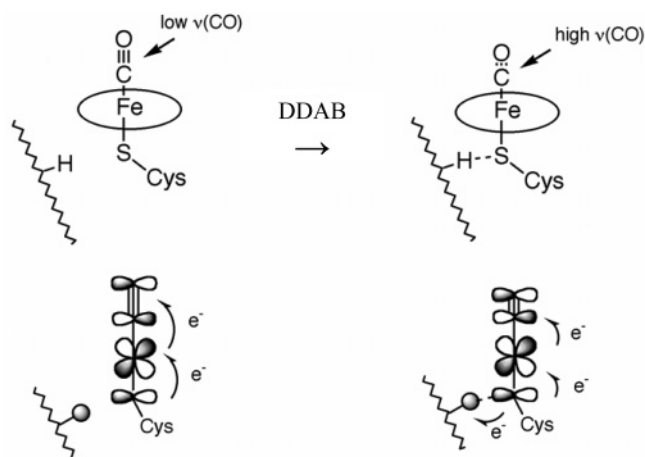(50) Battistuzzi, G.; Borsari, M.; Cowan, J. A.; Ranieri, A.; Sola, M. *J. Am. Chem. Soc.* **2002**, *124*, 5315−5324.
(51) Liu, X.; Huang, Y.; Zhang, W.; Fan, G.; Fan, C.; Li, G. *Langmuir* **2005**, *21*, 375−378.
(52) Poulos, T. L.; Finzel, B. C.; Howard, A. J. *Biochemistry* **1986**, *25*, 5314−5322.
(53) Tezcan, F. A.; Winkler, J. R.; Gray, H. B. *J. Am. Chem. Soc.* **1998**, *120*, 13383−13388.

Scheme 1

structure.[54,55] To test this prediction, we used IR absorption spectroscopy on the BM3 $Fe^{II}-CO$ adduct as a reporter of perturbations to the heme electronic environment. Prior work with the P450 ferrous carbonyl complex has established a range for this absorption maximum ($\sim1900-1950$ cm^{-1});[47,56] similar spectra recorded for BM3 yielded a value of 1950 cm^{-1} (Figure 6). As can be seen in Figure 6, DDAB causes the carbonyl stretching frequency to shift > 100 cm^{-1}.[57] This result implies a stronger $C-O$ bond in the BM3 $Fe^{II}-CO-DDAB$ system, which in turn indicates diminished π-back-bonding from the metal to the carbonyl ligand (Scheme 1). This observation is consistent with increased hydrogen bonding to the heme axial cysteine, as proposed for P420, which would weaken the iron–thiolate interaction and in turn result in decreased electron density at the metal center. The end result would be an even further positive shift in the heme reduction potential (diminished "push" effect), thereby affecting the catalytic activity of the enzyme.[54,55,58,59]

Our electrochemical and spectroscopic work sheds new light on the origin of the large positive potential shifts that accompany encapsulation of heme-thiolate proteins in surfactant films. First, there is the hydrophobic effect. Significant dehydration of the protein likely occurs within the bilayer environment, resulting in hydrophobic collapse and stabilization of the Fe^{II} (five-coordinate) heme. Second, our proposal of enhanced H-bonding resulting in a P420-like state would further stabilize the ferrous enzyme, once again increasing the heme redox potential. Notably, our model is fully consistent with recent surface-enhanced resonance Raman investigations by Todorovic et al., which suggest that immobilization of P450 on modified silver surfaces perturbs the heme potential by dehydration and by decreasing the electron donor strength of the heme axial thiolate, ultimately producing P420.[60]

Our results also provide plausible explanations for two long-standing questions. First, there is the very small increase in heme redox potential in the presence of CO for voltammograms recorded for P450–DDAB systems (typically $< +100$ mV). The dramatic stabilization of the ferrous state coupled with a weakened heme–carbonyl interaction produces a system where the added benefits of heme π-back-bonding to CO are greatly diminished. Second, regarding the lack of electrode-driven oxidative catalysis, our results suggest that BM3–DDAB film systems will not be successful at achieving substrate turnover due to the apparent P420-like state of the enzyme. The profound effect of H-bonding on the heme axial thiolate, modulations of this H-bonding through interactions with various "effectors" in the native system (e.g., reductase proteins[56,61]), and the resulting subtle perturbations to the heme redox potential all imply that a system where these interactions are disrupted from the finely tuned native system will fail to function. Indeed, the poor catalytic activity (cf. native activity) displayed by P450–DDAB systems supports this claim.

Our findings for BM3 will likely be applicable to some extent to all heme protein–surfactant systems. Conceivably, a protein that already possesses a rigid structure (e.g., P450 from *Sulfolobus solfataricus*) may not exhibit the behavior we have observed with BM3, while other more flexible proteins (e.g., mammalian P450s) may display even more dramatic changes associated with perturbations of the heme environment. The nature of the surfactant and the features of the supporting electrolyte (e.g., pH, counterions) also are likely to have an important effect on the observed properties of the protein; indeed, a systematic study with CAM illustrates this point,[12] as do our own results with BM3 under different conditions.[62]

Materials and Methods

Protein Expression and Purification. Expression and purification of the heme domain of BM3 with a C-terminal (His)$_6$ tag proceeded as previously described.[63]

Films for Voltammetry. Buffers for all experiments consisted of 50 mM KP$_i$/50 mM KCl/pH 7, unless otherwise stated. Hemin chloride was purchased from Porphyrin Products, Inc. (UT).

Electrodes for voltammetry (0.07 cm^2) were made using the basal plane of pyrolytic graphite. The surfaces were prepared by sanding lightly with 600-grid sandpaper, followed by polishing with 0.3 and 0.05 μm alumina slurries. The electrodes were then sonicated and dried in air. DDAB films were formed by placing 5 μL of 10 mM aqueous DDAB on the surface of the electrodes, followed by slow drying in air overnight. BM3 was incorporated into the film by soaking the DDAB-filmed electrode in a solution of enzyme (~20 μM in 50 mM KP$_i$ pH 7 buffer) for 20 min at ambient temperature, followed by gentle rinsing with double-distilled H$_2$O. Analogous films with hemin were made by soaking DDAB-filmed electrodes in a 50 μM solution of hemin chloride in buffer for 20 min.

A CH Instruments Electrochemical Workstation system was used for voltammetry measurements. Experiments at ambient temperature

(54) Yoshioka, S.; Takahashi, S.; Ishimori, K.; Morishima, I. *J. Inorg. Biochem.* **2000**, *81*, 141−151.

(55) Ost, T. W. B.; Clark, J.; Mowat, C. G.; Miles, C. S.; Walkinshaw, M. D.; Reid, G. A.; Chapman, S. K.; Daff, S. *J. Am. Chem. Soc.* **2003**, *125*, 15010−15020.

(56) Nagano, S.; Shimada, H.; Tarumi, A.; Hishiki, T.; Kimata-Ariga, Y.; Egawa, T.; Suematsu, M.; Park, S.-Y.; Adachi, S.; Shiro, Y.; Ishimura, Y. *Biochemistry* **2003**, *42*, 14507−14514.

(57) Notably, preliminary IR spectra in specular reflectance mode of BM3 $Fe^{II}-$CO in DDAB films on glassy carbon reveal a peak at 2050 cm^{-1}, similar to the peak position observed in DDAB dispersions.

(58) Low, D. W.; Hill, M. G. *J. Am. Chem. Soc.* **2000**, *122*, 11039−11040.

(59) Shaik, S.; Kumar, D.; de Visser, S. P.; Altun, A.; Thiel, W. *Chem. Rev.* **2005**, *105*, 2279−2328.

(60) Todorovic, S.; Jung, C.; Hildebrandt, P.; Murgida, D. H. *J. Biol. Inorg. Chem.* **2006**, *11*, 119−127.

(61) Glascock, M. C.; Ballou, D. P.; Dawson, J. H. *J. Biol. Chem.* **2005**, *280*, 42134−42141.

(62) The effect of the counterion was probed in BM3−DDAB experiments in the presence of sodium bromide: while the difference spectrum of the $Fe^{II}-$CO complex shows the same time-dependent conversion of P450 to P420, voltammetry yields broader, less intense peak currents. Our work with BM3 in sodium dodecyl sulfate films also is relevant: the $Fe^{III/II}$ redox potential is −330 mV (vs Ag/AgCl, pH 7.4), and catalytic reduction of dioxygen is observed (submitted to Langmuir April 2006).

(63) Cirino, P. C.; Arnold, F. H. *Adv. Synth. Catal.* **2002**, *344* (9), 1−6.

were performed in a two-compartment cell, using a platinum wire auxiliary and an SCE reference electrode. All experiments were performed under argon in thoroughly degassed buffer unless otherwise stated. Experiments at variable temperature were conducted in a three-neck flask. Working and counter electrodes were placed directly into solution (~5 mL), while the SCE reference electrode was separated by a Luggin capillary. The temperature of the flask was controlled by placing the electrochemical cell in a thermostated ethylene glycol bath (18.5−40 °C, ±0.1°C), while the temperature was monitored with a thermocouple placed directly into the flask. The reference electrode was held at constant (room) temperature, connected to the thermostated cell with a salt bridge.

Films for Absorption Spectroscopy. BM3−DDAB films on surfaces for absorption spectroscopy were prepared on 3.5 × 40 mm² fused silica slides. The slides were made hydrophobic by coating with (3-mercaptopropyl)trimethoxysilane using the following protocol. The silica slides were cleaned by boiling in piranha solution (4:1 H_2SO_4/ 50% H_2O_2) for 20 min followed by rinsing with double-distilled H_2O. The following procedure[37] was then performed 3 times: the slides were placed in a 40:1:1 refluxing solution of 2-propanol/double-distilled H_2O/ (3-mercaptopropyl)trimethoxysilane for 10 min, washed with 2-propanol, and then baked in a 100−107 °C oven for 10 min. BM3−DDAB films were cast onto the slides by placing 50 μL of 100 μM BM3 and 70 μL of 10 mM DDAB in double-distilled H_2O onto the glass slide, followed by drying in air overnight. Slides for negative controls were filmed with DDAB only. Absorption spectra were recorded with a Hewlett-Packard spectrophotometer by placing the silica slides in a cuvette. The absorption spectrum shown in Figure 1 is a difference spectrum of slides with and without BM3.

Electronic Absorption Spectroscopy in Solution. Absorption spectra were recorded with a Hewlett-Packard spectrophotometer at ambient temperature. The BM3 Fe^{II}−CO adduct was generated by adding a small scoop of sodium dithionite powder to 2 mL of BM3 (2 μM) in buffer, followed by bubbling CO through the solution. To 500 μL of this solution, 2 μL of 10 mM DDAB in water were added. Absorption spectra were then recorded at 5 min intervals. Analogous time-dependent absorption spectra were recorded for hemin (25 μM) with DDAB (40 μM) in buffer. The difference spectrum (Figure 2b) was recorded by making a solution of the BM3 Fe^{II}−CO adduct (1.3 μM) with DDAB (40 μM), immediately using this solution to blank the spectrophotometer, and then recording absorption spectra of this same solution at various time intervals.

Infrared Absorption Spectroscopy. Infrared spectra were recorded using a Nicolet FTIR instrument with a liquid-nitrogen-cooled MCT detector. The IR cell consisted of calcium fluoride windows and a 0.025 mm Teflon spacer.

The samples for the spectra in Figure 6 were prepared as follows. The buffer used was 50 mM KP_i pH 7. For the sample containing DDAB, 100 μL of a 10 mg/mL sodium dithionite solution, 50 μL of a 400 μM BM3 solution, and 50 μL of a 10 mM DDAB solution were mixed. The mixture was placed into a sealed flask, and CO was introduced to the sample by evacuating the flask and backfilling with pure CO; this was performed several times. The sample in the absence of DDAB was prepared in the same way, except no DDAB was added.

Supporting Information Available: Electronic absorption spectra of hemin and hemin−DDAB mixtures, a cyclic voltammogram of hemin in DDAB on graphite and the resulting hemin $E_{1/2}$ vs temperature plot. These materials are available free of charge via the Internet at http://pubs.acs.org.

JA061896W